Correlations between Function and Dynamics: Time Scale Coincidence for Ion Translocation and Molecular Dynamics in the Gramicidin Channel Backbone†

C. L. North‡ and T. A. Cross*

National High Magnetic Field Laboratory, Institute of Molecular Biophysics and Department of Chemistry, Florida State University, Tallahassee, Florida 32306

Received November 10, 1994; Revised Manuscript Received February 27, 1995⊗

ABSTRACT: The polypeptide backbone of gramicidin lines the channel lumen, which maintains a single file string of water molecules and the occasional cation. Whether or not local motions of the backbone are important for facilitating cation transport has been the subject of debate. Here it is demonstrated that motions of the backbone occur on the same time scale as cation translation through this transmembrane channel. To characterize the frequency of the local motions, field-dependent ^{15}N T_1 relaxation times were interpreted in light of an independently determined motional model that defines the motions as occurring about the $C_\alpha-C_\alpha$ axis. To overdamp these local motions, several models that involve extensive correlations of the molecular motions were considered. One of these schemes for correlated motions suggests a unidirectional reaction path that would minimize the time necessary for the cation to pass through the low-dielectric center of the bilayer.

Molecular dynamics are essential for functional processes, and their characterization has been approached both computationally and experimentally. Motion in the polypeptide backbone is often restricted to small amplitude librational motions which have been predicted (McCammon & Harvey, 1987) but rarely defined by experiment. Whether these librations are integral or incidental to protein function is dependent on the specific functional role of the macromolecule. For nonstructural proteins the flexibility of the backbone may be important for catalysis, binding, transport, or other functional activities.

Due to its functionality, size, and accessibility, the transmembrane ion conducting channel formed by gramicidin A has been extensively studied (Killian, 1992; Busath, 1993; Cross, 1994). Gramicidin's channel formation, lifetime, and conductance are well characterized in a range of model membrane environments and for numerous sequence mutations (Fonseca et al., 1992; Koeppe et al., 1990; Becker et al., 1992). Computational studies of the channel's structure and dynamics have provided a wealth of information to draw upon for generating models (Woolf & Roux, 1994; Busath & Szabo, 1981; Chiu et al., 1993). This literature provides a unique opportunity for testing the computational methods with a high-resolution experimental characterization of dynamics. Fundamental questions about channel efficiency, conductance pathway, and kinetic models for cation translocation are all dependent on a high-resolution structure and dynamics characterization. In this channel the backbone atoms provide much of the solvation environment for the cations, and therefore the backbone motions may play a direct role in cation transport (Venkatachalam & Urry, 1984; Chiu et al., 1991; Roux & Karplus, 1991b; North & Cross, 1993).

Solid state NMR offers a powerful approach for measuring the rates and amplitudes of localized polypeptide backbone motions. The opportunity to observe averaging of nuclear spin interactions provides a mechanism to characterize a model for the local motions of a specific site. In contrast, solution-state relaxation data require an assumed model for the molecular motions. Furthermore, global molecular reorientation often provides very efficient nuclear spin relaxation in solution. In solid-state NMR, global motions are restricted in anisotropic environments and may not provide an efficient relaxation mechanism. Consequently, spin−lattice relaxation parameters are more sensitive to local motions in solid-state spectroscopy than in the solution-state analog. Spectral densities for local fluctuations can be approximated as functions of the experimentally determined model parameters. In this way, molecular motions can be related directly to the relaxation observations. Spin−lattice relaxation, T_1, for an amide ^{15}N site is almost exclusively due to oscillating local fields generated by the motions of the dipolar interaction with the covalently linked proton. Both characteristic times and amplitudes of molecular motions can be deduced from measurements of magnetic field strength dependent spin−lattice relaxation.

The primary structure of gramicidin A is (Sarges & Witkop, 1965):

HCO-L-Val_1-Gly-Ala_3-D-Leu_4-L-Ala_5-D-Val_6-L-Val_7-D-Val_8-L-Trp_9-D-Leu_{10}-L-Trp_{11}-D-Leu_{12}-L-Trp_{13}-D-Leu_{14}-L-Trp_{15}-$NHCH_2CH_2OH$

The high-resolution three-dimensional backbone structure of the gramicidin A channel in dimyristoylphosphatidylcholine (DMPC)[1] bilayers has been determined experimentally (Ketchem et al., 1993). The orientation of numerous

† This work has been supported by the National Institutes of Health (No. AI23007) and the National High Magnetic Field Laboratory.

‡ Present address: Department of Chemistry, University of Virginia, Charlottesville, VA 22901.

⊗ Abstract published in *Advance ACS Abstracts,* April 15, 1995.

[1] Abbreviations: DMPC, dimyristoylphosphatidylcholine; HPLC, high-performance liquid chromatography; rms, root mean square; SDS, sodium dodecyl sulfate; NOE, nuclear Overhauser effect; PBG, poly(benzyl glutamate).

0006-2960/95/0434-5883$09.00/0

internuclear bond vectors with respect to the helix axis was measured using solid-state NMR of uniformly aligned samples of isotopically labeled gramicidin A. By combining this information with constraints from the covalent bond geometry, the conformation of the peptide backbone was achieved. More recently, all of the side-chain conformations have been deduced using a similar approach (Hu et al., 1993; Lee & Cross, 1994; Koeppe et al., 1994; Lee et al., 1995).

The channel structure is a helix with 6.3 residues per turn giving it a length of approximately 26 Å and a pore diameter of approximately 4 Å. It conforms to the β-helical motif proposed by Urry (1971) although it is right-handed as shown by Nicholson and Cross (1989) and Arseniev et al. (1986). This structure places all side chains in contact with the lipid environment and the peptide backbone lines the channel lumen that supports a single-file column of water molecules. The axis connecting successive α-carbons, the $C_\alpha-C_\alpha$ axis, that determines the local pitch of the helix alternates between an angle of approximately 8° and 15° with respect to the plane of the bilayer.

On the basis of ^2H relaxation measurements of d_5-deuterated $Trp_{9,11,13,15}$ gramicidin A, Macdonald and Seelig (1988) estimated that the global correlation time for the channel in DMPC at 55 °C is 200 ns. This evaluation assumed that the local motions of the indole rings did not significantly relax the quadrupolar spins. Recent results indicate that while there is no rotameric isomerization of the tryptophan side chains (Hu et al., 1993), there is substantial librational motions of the indole ring (Hu, 1994). The global correlation time for the channel conformation in DMPC bilayers has now been fully characterized as a function of temperature through the gel to liquid-crystalline phase transition temperature range (Lee et al., 1993). These experiments were performed on d_4-Ala_3 gramicidin A and d_4-Ala_5 gramicidin A. The global correlation time was determined by simulating ^2H quadrupole echo line shapes that showed intermediate time frame averaging. Such line shapes dictate motional frequencies in or near the microsecond time scale. This previous study documents that the global correlation time is 1.0 μs at 309 K and 3.3 μs at 301 K, this latter temperature being close to that used for the relaxation studies reported here. It also showed a loss of the intermediate timeframe averaging at 52 °C which was interpreted as a correlation time of less than or equal to 330 ns (Lee, 1994).[2]

Spatial characteristics of the local backbone dynamics have been studied by ^{15}N solid-state NMR of gramicidin A in DMPC bilayers (Lazo et al., 1993, 1995). Single site amide ^{15}N labeled gramicidin A in hydrated DMPC bilayers was fast frozen in liquid propane to avoid conformational heterogeneity induced by the bilayer phase transition and ice crystallization (Evans et al., 1993). The well defined static powder pattern spectra observed below 200 K are averaged by molecular motions above this temperature and below 288 K when global reorientation of the channel significantly affects the line shape. Anisotropic local averaging of the tensor was observed with only two of the three tensor elements significantly averaged. Such averaging was shown to be consistent with librational motions about the $C_\alpha-C_\alpha$ axis (Lazo et al., 1993, 1995).

Motions of peptide linkage planes in proteins and polypeptides are permitted through rotations about the bonds on either side of the α-carbons, designated by the dihedral angles ϕ and ψ. Such motions which do not significantly alter the overall structure of a peptide are termed librations (Urry et al., 1985). It has been suggested that peptide plane librations are responsible for rotating the backbone carbonyl groups into the channel lumen to provide a solvation environment for translocating cations as an important part of the mechanism for ion transport (Urry et al., 1981; Mackay et al., 1984; Venkatachalam & Urry, 1984; Roux & Karplus, 1991a,b). Solvating a bound cation in this manner lowers the energy barrier required to strip four of the six waters in its primary hydration shell as it enters the narrow pore. Bifurcated hydrogen bonds to the carbonyl oxygens have been computationally predicted in this channel and experimentally observed in several macromolecular systems (Chiu et al., 1989). It has been suggested that peptide plane librations could provide a mechanism for passing ions and water molecules between local minima in the potential energy profile of the channel (Roux & Karplus, 1991a,b).

Localized dynamics in polypeptides have been studied experimentally and modeled computationally. The typical range of characteristic times for rotations of side chains on the protein surface is calculated as 10−100 picoseconds. For librations of groups on the interior of globular proteins, a range of 10 ps to 1 ns is typical (McCammon & Harvey, 1987). Motions in proteins may be underdamped, as in the vibrations of bonds or twisting of the peptide plane, or overdamped as in the motions of large hydrophobic groups. A simple calculation for the oscillation frequency of a planar unit with the rotational moment of inertia of a peptide plane about an axis through successive α-carbons restricted by a harmonic potential to a small amplitude gives a period of less than a picosecond (Usha et al., 1991). Roux and Karplus (1988) and Brooks and Karplus (1983) found that the rms ϕ and ψ dihedral angle fluctuations were approximately 10° for both the L- and D-amino acid residues. The lowest frequency fluctuations were relatively short-range correlated backbone motions occurring at frequencies between 20 and 4.6 cm^{-1}. These frequencies correspond to an approximate range of harmonic oscillator periods from 2 to 8 ps. However, normal mode analysis ignores solvent effects and does not model anharmonic potentials which have been shown to result in longer correlation times in molecular dynamics simulations.

A number of early microscopic approaches to modeling the free energy profile of ions in the channel were attempted to explain conductance and selectivity of the gramicidin channel [reviewed by Jordan (1987)]. Calculating the free energy profile amounts to calculating the reversible work required to move an ion through the channel. One model

[2] The correlation time for the gramicidin channel global motion was reported as 36 μs (Lee et al., 1993) using a nonstandard autocorrelation function. 36 μs represents the period in which the RMS rotational displacement is one turn. The conventional correlation time is calculated as follows: The rotational diffusion of the global motion was modeled as an N-state jump motion with $N = 36$. The rotational diffusion constant is $D = 2\pi k/N^2$ rad/s, where k equals the jump rate between states. The jump rate was correctly determined to be 4.5×10^7 Hz from Ala-3 data and 3.0×10^7 from the Ala-5 data. The conventional global correlation time, τ_p, is defined as $(6D)^{-1}$. Therefore, the value of τ_p should have been reported as 0.8 μs for the Ala-3 data and 1.2 μs for the Ala-5 data for an average 1.0 μs at 309 K. These latter calculations are consistent with the calculations derived from the correlation function for N-equivalent states with nearest-neighbor jumps (Torchia & Szabo, 1982).

developed by Jordan and co-workers (Lee & Jordan, 1984; Sung & Jordan, 1987a,b) provided for a flexible polyglycine backbone as an ion passes through the channel. A proposed pathway through the channel shows a number of local energy minima along with an ion binding site near the Trp_{11} C=O. This model reproduces some of the observed properties of the gramicidin channel; however, the energy of translocation is larger than can be accounted for by the permeation rate. Furthermore, this model and others have assumed that on the time scale of ion translocation a constant time-average potential surface would present itself to the ion.

More recently, the potential of mean force as a function of position in the interior of an infinite periodic poly(L,D-alanine) β-helix model channel was calculated for Na^+ and K^+ (Roux & Karplus, 1991a,b). For this study a full molecular dynamics simulation was performed as an ion was moved stepwise through the model channel. Channel waters were included, but not the lipid environment. In the model, water molecules in an ion free channel associated with each other and with C=O groups which librated into the channel. With a Na^+ ion in the channel regular binding sites were found, one site for every two carbonyl oxygens. Libration of carbonyl groups into the channel allowed an ion to maintain a solvation environment while in the channel. The perturbation in structure caused by the presence of an ion extended 4−6 residues, limited by the flexibility of the helix. This demonstrated a strong local cooperativity in structural perturbations. The rms librational amplitudes for all residues of the channel were 15−20° with the presence of an ion causing the mean position to change by as much as 30° locally. In the simulation, backbone librations occurred on the picosecond time scale, 75−150 cm^{-1} in agreement with the normal mode study which found librations at this frequency and amplitude (Roux & Karplus, 1988). The acquisition time of the simulation at each point of the ionic trajectory was limited to 25 ps, and the structure was seen to relax in the presence of an ion in less than 20 ps. It was shown that the periodic energy minima were not separate. This suggests that an ion does not jump from rigid site; to rigid site, rather the structure is plastic so that a helix distortion follows an ion and keeps it solvated.

Other recent molecular dynamics simulations of the gramicidin channel have been performed which again predict significant backbone and side chain motions on the picosecond time scale (Chiu et al., 1989, 1991, 1993; Woolf et al., 1995). A systematic tendency for the C=O groups to bend into the channel lumen allowing hydrogen-bonding to channel waters was observed. The bonding restrained both translational and rotational water mobility. The studies have confirmed the highly correlated nature of water in the channel. These simulations are limited to times <300 ps and have also ignored the lipid environment in favor of artificial restraints on the channel structure. Chiu and Jakobson (1993) have found collective periodic damped motions of the gramicidin backbone in time-correlation analyses of their molecular dynamics simulations. The period of these motions was on the picosecond time scale, and correlation lasted tens of picoseconds. The simulation again did not include an explicit lipid environment for the channel.

In this study, the rates and amplitudes of motions of several amide sites along the gramicidin channel backbone have been determined from solid-state NMR spin−lattice relaxation T_1 times. Field-dependent T_1 relaxation times are interpreted in light of structural models of the motion which account for what is known of the structure and dynamics of the gramicidin A channel backbone. The results demonstrate that there are motions in the gramicidin channel backbone which occur on the order of nanoseconds. These motions occur on the same time scale as ion translocation events raising the possibility of a direct relationship between dynamics and function.

MATERIALS AND METHODS

Isotopically labeled L- and DL-amino acids were purchased from Cambridge Isotope Labs (Woburn, MA). For labeled D-amino acids the racemic mixture was purchased and resolved by an enzymatic process (Teng & Cross, 1989). Gramicidin was synthesized by solid-phase peptide synthesis with Fmoc chemistry as described previously (Harold & Baarada, 1967; Fields et al., 1989). In addition to the ^{15}N D-Leu_4 site studied previously (North & Cross, 1993), ^{15}N isotopic labels were incorporated in the backbone amides of residues Gly_2, D-Val_8, and Trp_9 in one synthesis and in residues D-Val_6, D-Leu_{12}, and Trp_{13} individually. These samples were purified by semipreparative reverse-phase HPLC as described previously (Fields et al., 1989).

Oriented samples of amide ^{15}N-labeled gramicidin A channels in hydrated DMPC lipid bilayers were prepared between glass coverslips by first codissolving ~170 mg of lipid and peptide (8:1 by moles) in 300 μL of MeOH/H_2O (95:5 by volume). After the solution was spread onto 18 coverslips (cut 22 × 5 mm with adhesive spacers at each end), the samples were dried, stacked, hydrated to saturation, and sealed in a 25 × 6 × 6 mm glass tube and then allowed to anneal at 45 °C for at least 7 days as previously described (North & Cross, 1993). The coverslip normal and consequently the bilayer normal and channel axis were all aligned parallel to the magnetic field for the relaxation measurements. Very uniform orientation of the lipid bilayers and channels can be achieved by this method (Moll & Cross, 1990; Cross et al., 1992).

^{15}N spin−lattice relaxation measurements were obtained at 4.7 and 9.4 T corresponding to 20 and 40 MHz for the ^{15}N frequencies. The lower field spectrometer utilized a 51 mm bore Oxford magnet and an IBM/Bruker console with a Doty Scientific solids package. This instrument has been heavily modified to improve performance (Nicholson et al., 1987). The higher field instrument includes an Oxford Instruments 89 mm bore magnet, a Chemagnetics data acquisition system, and home-built RF electronics. A modification of the cross-polarization T_1 (CPT1) experiment was used to make the measurements. As proposed by Torchia (1978), the CPT1 experiment utilizes the increased strength of observed resonances prepared by cross-polarization before measuring spin−lattice relaxation by inversion−recovery. In our modified version, proton magnetization is returned to the ^+Z axis following cross-polarization rather than being saturated by a low level continuous pulse during the inversion−recovery phase of the experiment. A Hahn echo (τ_{HE} = 48 μs) sequence was also used to avoid probe ringing problems. Ninety degree pulses were approximately 6.6 μs, and a 1 ms mixing time and a 7s recycle delay were used.

Description of Motional Models. To interpret the spin−lattice relaxation data, two specific motional models were

developed based on independent experimental data. The models contain a minimum number of adjustable parameters in order to avoid overinterpretation. The axis of global reorientation has been shown to be parallel to the bilayer normal (Smith & Cornell, 1986; Fields et al., 1988). Furthermore, the channel, helical, and motional axes are all parallel to each other and for the samples studied here these axes are aligned parallel to the magnetic field direction. The rate of global molecular reorientation has been accurately determined as a function of temperature by ^{2}H powder pattern analysis of gramicidin in hydrated lipid bilayers (Lee et al., 1993). This global motion is characterized by a single exponential and a unique correlation time, τ_p. For the gramicidin channel there is specific structural information available about the local motions in the polypeptide backbone. These local motions have been shown to occur about the $C_\alpha-C_\alpha$ axis (Nicholson et al., 1991). Furthermore, from the high-resolution structure of the channel (Ketchem et al., 1993) the orientation of this axis and the mean orientation of the peptide plane about the $C_\alpha-C_\alpha$ axis are known with respect to the channel axis.

In the first model, the "sweep" model, the N−H vector librates about a precisely defined $C_\alpha-C_\alpha$ axis with motions modeled by rotational diffusion subject to a harmonic potential driven by Brownian collisions. The autocorrelation functions of such a restricted diffusional motion can be acceptably approximated by an exponential decay as shown by Lipari and Szabo (1981, 1982a,b). Therefore, the correlation function is approximated by a single exponential characterized by a correlation time and the amplitude of the equilibrium distribution of displacements from the mean peptide plane position. In this "sweep" model the polar coordinates of the interaction vector in the laboratory reference frame, θ_χ and ϕ_χ, are functions of a fixed tilt of the $C_\alpha-C_\alpha$ axis, the mean rotation of the peptide plane about the $C_\alpha-C_\alpha$ axis, and the rotational displacement, χ. The functions θ_χ and ϕ_χ have been derived from rotation matrices that transform the position of the ^{15}N−^{1}H vector of an arbitrarily oriented peptide plane into the lab frame. The tilt and mean rotation have been determined by previous solid state NMR experiments and are not variables. Therefore, in this model θ_χ and ϕ_χ trace a precise arc swept out by the N−H vector resulting in a root mean square (rms) amplitude and a characteristic time for the local motions as the sole variables. The amplitude and equilibrium distribution of the local displacements are determined by the potential well which restricts local motions. Here, the application of a harmonic restoring potential results in a Gaussian distribution of diffusive displacements (Chandrasekhar, 1943). A harmonic restoring potential is well supported on theoretical and experimental evidence (McCammon & Harvey, 1987). The resulting Gaussian distribution is commonly used in modeling molecular dynamics and is the basis for normal mode analysis. Interpreting the relaxation data in light of this model has the advantage of including in the analysis all that is presently understood about the structure and dynamics of the system. However, this model is perhaps more restrictive than can be justified; there is no justification for a single rigidly fixed axis for local motions and no proof that another probability distribution for displacements about the mean is not more appropriate, such as an asymmetric distribution. Consequently, interpretation of the relaxation data in light of this model in order to obtain precise physical parameters of local motion may lead to conclusions which are not entirely warranted.

The second model differs in the manner in which the N−H vector is allowed to librate. This "wobble" model more loosely confines the libration within a rectangular pyramid, akin to the "wobble in a cone" model (Bull, 1978; London, 1980). Because the $C_\alpha-C_\alpha$ axis is nearly perpendicular to the channel axis, local librations about the $C_\alpha-C_\alpha$ axis result primarily in changes to the polar angle θ of the N−H bond with respect to the helix axis. The dimensions of the librational range have been set to favor motions about the axis rather than of the $C_\alpha-C_\alpha$ axis by a ratio of 10:1 for the pyramidal base defined by the polar angles, θ_w and ϕ_w. In other words, the interaction vector is allowed to librate independently through amplitudes $\pm\theta_w$ and $\pm\phi_w$ on either side of the mean position of the N−H vector. The equilibrium distribution of displacements from the mean position used in this model is akin to the wobble in a cone model. It has been found in many molecular dynamics simulations that near the surface of proteins motions are anharmonic and do not display a Gaussian distribution; rather, the restricting potential is formed by hard steric constraints (McCammon & Harvey, 1987). For this reason, a square-well potential producing a constant distribution within fixed amplitudes is considered for this model. This approach is somewhat less satisfying because the physical parameters obtained from such an analysis are more qualitative in nature. However, this model may be more realistic.

The basic form of the correlation functions for both models is similar to the "wobble in a cone" model proposed by Bull (1978) and adapted for oriented samples by North and Cross (1993). The difference between the analyses using these two models appears in small variations in the values of the correlation function at $t = 0$ and in the magnitude of the correlation which decays due to local motion for a given amplitude, $C(0)$ and $[C(0) - C(t > \tau_i)]$. Evaluation of the constants $C(0)$ and $C(t > \tau_i)$ depend on the spatial characteristics of the local motions and an appropriate equilibrium distribution.

Calculation of T_1 Times. Theoretical T_1 times are calculated as functions of the parameters of molecular motions as shown in North and Cross (1993). Autocorrelation functions of the F^q terms of the dipolar Hamiltonian as given by Abragam (1961) are approximated in the manner suggested by Bull (1978). Fourier transforms of these correlation functions give the model spectral densities which lead directly to theoretical T_1 times as functions of the model motional parameters. The F^q terms are

$$F^0 = 1 - 3\cos^2\theta$$

$$F^1 = \sin\theta\cos\theta\exp(-i\phi)$$

$$F^2 = \sin^2\theta\exp(-2i\phi) \quad (1)$$

Since the global and local motions are considered independent, the correlation functions are approximated by a sum of exponential decays. In the first short period, a fraction of the total amplitude of the correlation function at $t = 0$ decays due to the faster localized motions with a limited contribution from the slower global molecular reorientation. After $t > \tau_i$, the remaining degree of correlation decays with the characteristic time of global molecular reorientation alone.

Assuming that the global diffusion and localized motions are not correlated and that $\tau_i \ll \tau_p$ allows us to claim that we know the value of $C(t)$ at three points. At $t = 0$,

$$C(0) = \int P(\Omega) F_q(0) F_{-q}(0)\, d\Omega$$

which is

$$C(0) = \int P(\Omega) |F_q(0)|^2\, d\Omega \quad (2)$$

where the integration is over the equilibrium distribution of molecular positions. At some time longer than τ_i but shorter than τ_p the interaction vector may have moved internally to a new position, but since the system is stationary, the distribution probability remains constant. In this initial period of time (much less than τ_p), the molecule will not have reoriented globally to any noticeable extent. At this point,

$$C(t) = \int\int P(\Omega_0) F_q(\Omega_0) P(\Omega_t|\Omega_0) F_q(\Omega_t)\, d\Omega_0\, d\Omega_t$$

which is

$$C(t) = |\int P(\Omega) F_q(0)\, d\Omega|^2 \quad (3)$$

The difference between these terms is proportional to the average change in the dipolar interaction energy when the interaction vector moves from any position in the equilibrium distribution to any other position in the equilibrium distribution due to local motions. The remaining amplitude of the correlation function decays to zero with the characteristic time of global reorientation. However, in the case where the global rotation is about the magnetic field axis, F_0 is unaffected so that $C_0(t)$ decays only with the characteristic time τ_i. This is the case in our samples.

In evaluating $C(0)$ and $C(t > \tau_i)$, most authors have used Wigner rotation matrices to transform the $F_q(\theta,\phi)$ functions from a local molecular reference frame into the laboratory frame. The F_q functions are closely related to spherical harmonics which appear in the equations of angular momentum, and the Wigner terms allow for the rotation of the functions themselves. This is convenient in many cases because in integrating over all orientations, as in solution studies, certain rules apply which simplify the calculations considerably. Because of the uniform orientation of the gramicidin channels in the laboratory frame, it is more convenient here to express the orientation of the interaction vector directly in the laboratory reference frame before evaluating F_q. In the case of the wobble model all that is needed is the average angle that the interaction vector makes with the channel and field axes and the range of motion. The choice of $\phi_{(t=0)}$ is arbitrarily zero. The F_q can be directly integrated over the rectangular region to which local motion is restricted.

For the sweep model, θ_χ and ϕ_χ are expressed as functions of tilt and mean rotation of the C_α–C_α axis $\pm\chi$. To evaluate θ_χ and ϕ_χ, a simple scheme of Euler rotation matrices were used to transform a unit interaction vector from an arbitrary reference frame to the lab reference frame as a function of tilt and rotation. The resulting vector provides the cosine and sine of θ and ϕ as a function of the structural and displacement parameters.

After numerically evaluating the constants, $C(0)$ and $C(t > \tau_i)$, the total correlation function is approximated by

$$C(t) = [C(0) - C(t > \tau_i)] \exp(-t(\tau_i^{-1} + \tau_0^{-1})) + [C(t > \tau_i) - C(\infty)] \exp(-t/\tau_0) + C(\infty) \quad (4)$$

The resulting spectral densities are

$$J^q(\omega) = FT[C^q(t)]$$

$$J^0(\omega) = \{C_i^0(0) - C_i^0(t > \tau_i)\}\left(\frac{2\tau_i}{1 + \omega^2\tau_i^2}\right)$$

and

$$J^q(\omega) = \{C_i^0(0) - C_i^0(t > \tau_i)\}\left(\frac{2(\tau_i^{-1} + q^2\tau_p^{-1})^{-1}}{1 + \omega^2(\tau_i^{-1} + q^2\tau_p^{-1})^{-2}}\right) + C_i^0(t > \tau_i)\left(\frac{2q^{-2}\tau_p}{1 + \omega^2 q^{-2}\tau_p^2}\right) \quad (5)$$

for $q = 1, 2$, which are substituted into the standard equation for T_1 relaxation of a spin by an unlike spin given by Abragam (1961):

$$\frac{1}{T_1} = \frac{3}{4}\frac{\lambda_I^2\lambda_S^2\hbar^2}{r^6}\left\{\frac{1}{12}J^0(\omega_I - \omega_S) + \frac{2}{3}J^1(\omega_I) + \frac{3}{4}J^2(\omega_I + \omega_S)\right\} \quad (6)$$

RESULTS

Figure 1 shows sample spectra from cross polarization T_1 experiments on ^{15}N[Gly$_2$, Val$_8$, Trp$_9$] gramicidin A obtained at 4.7 and 9.4 T. These data were collected from uniformly aligned preparations of the polypeptide in hydrated DMPC bilayers. The bilayer normal and channel axis were aligned parallel to the magnetic field. Because these amide nitrogen sites have different average orientations with respect to the channel axis, the chemical shift for each site is unique and well resolved in these spectra. Since each data set was recorded over a period of 3–5 days, the spectral sensitivity was verified by repeating the first experimental delay time in the last experiment. In all cases the intensity of the signal decreased by less than 20%. This reduction was probably due to the combined effects of instrumental detuning and degradation of the sample alignment. In calculating the T_1 times associated with each data set, the measured intensities were scaled according to the order of acquisition to account for this systematic signal degradation. The variable delay times were acquired in random order, thereby randomizing the residual systematic effects. Observed T_1 times and their associated error limits at 95% confidence are presented in Figure 2 as a function of the residue number. For those sites where duplicate data sets were obtained, the relaxation times were always reproducible within this statistical error range.

The ^{15}N T_1 times observed in this study are much shorter than spin–lattice relaxation times typically observed for amide nitrogens in anisotropic samples which can be several orders of magnitude longer. For example, T_1 for ^{15}N acetylglycine powder is 2000 s (Cross & Opella, 1982). This immediately suggests that motions exist in the system which occur at rates on the same order as the spin state transition frequencies. Also, the spin–lattice relaxation times display a field dependence; on average the relaxation times are

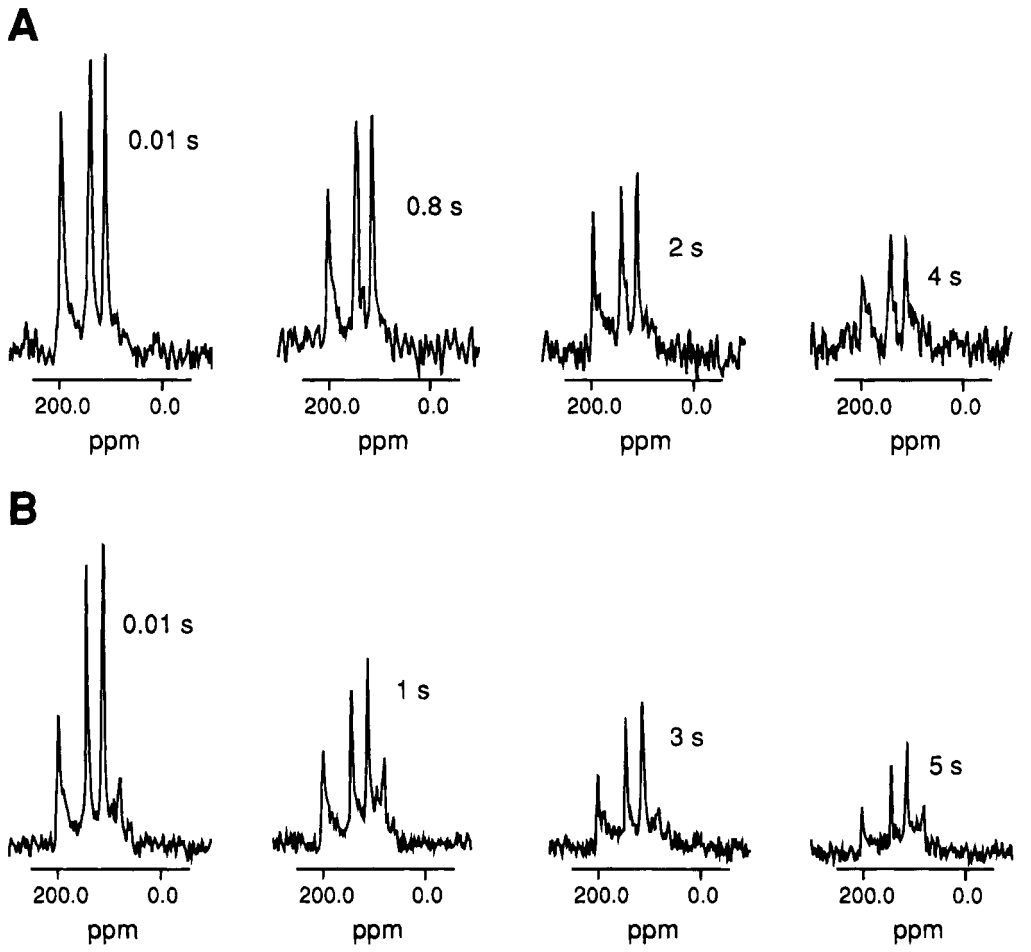

FIGURE 1: Sample spectra from ^{15}N T_1 experiments on oriented ^{15}N [Gly_2,Val_8,Trp_9]gramicidin A in hydrated DMPC at 302 K. Chemical shifts for Gly_2, Val_8, and Trp_9 are 113, 144, and 198 ppm, respectively, (A) at 4.7 T with T_1 delay times of 0.01, 0.8, 2, and 4 s, and (B) at 9.4 T with T_1 delay times of 0.01, 1, 3, and 5 s. Underlying powder pattern signals, most evident in the $\sigma_\perp$ signals at 60 and 80 ppm, results from sample that is not between the coverslips. The peak intensities were corrected for the powder pattern intensity.

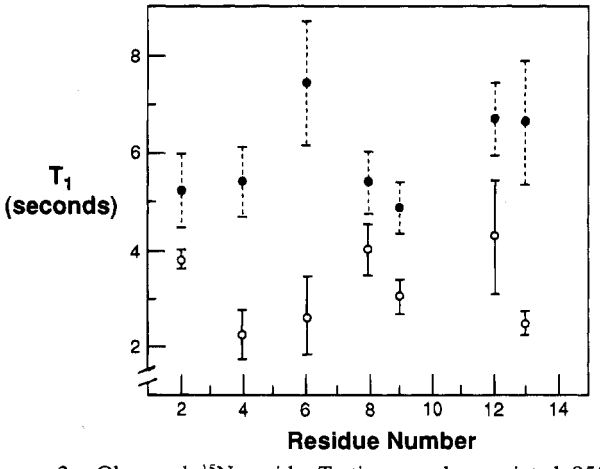

FIGURE 2: Observed ^{15}N amide T_1 times and associated 95% confidence limits for many backbone sites in the gramicidin A channel at 4.7 T (solid) and 9.4 T (dashed).

doubled at 9.4 T as compared to the data at 4.7 T. The field dependence would be absent if all motions were much faster than the interaction frequencies.

The relaxation times observed at a single field strength as a function of residue number suggest the possibility of dynamic variations along the channel axis; however, there are no significant trends in the relaxation times. Relaxation times for polypeptide sites at the bilayer surface are not systematically different from the relaxation times at the center of the bilayer as has been suggested for the backbone motion of the channel based on line width variation in aligned samples (Smith et al., 1989). However, it should be noted that the present study is primarily sensitive to motions on the nanosecond time scale and motions on other time scales might show such variations. The repeating structural unit in the gramicidin channel is a dipeptide, since the backbone conformation is a β-strand type of structure. Another pattern in dynamics might be anticipated for such a structure in which the dynamic amplitudes or frequency alternates along the sequence. Every other carbonyl oxygen is somewhat tipped in toward the channel axis (Ketchem et al., 1993) where it is available for solvating cations during transit through the channel. However, such an alternating pattern does not appear to be present in the experimental data.

In the analysis of the observed T_1 times the global correlation time was restricted to the 1 μs time scale in accordance with Lee et al. (1993). Motions on this time scale are sufficiently far from the transition frequencies involved in these experiments that they do not contribute greatly to the efficient relaxation that is observed. Additionally, with the global correlation time in the 1 μs range, the interpretation of this data is negligibly affected by the precise value of the global correlation time (North & Cross, 1993). While the global correlation time is temperature dependent, RF heating could affect the sample temperature even under

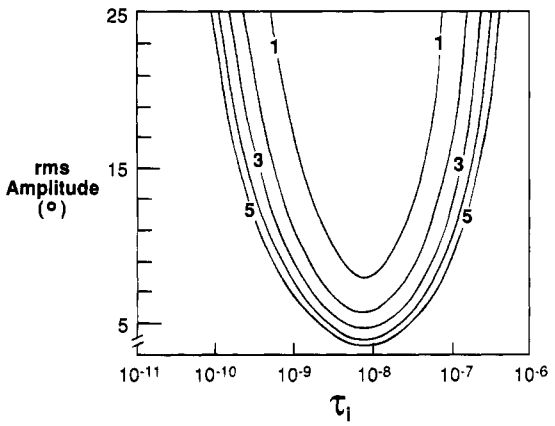

FIGURE 3: ^{15}N T_1 value contours as a function of local correlation time and local motional amplitude, as an rms angular deviation from mean. The data is from 4.7 T for the backbone amides with the average peptide plane orientations of the even numbered residues. The sweep model was used for the calculation of the T_1 values, and, therefore, the amplitude reflects an rms amplitude as a Gaussian distribution.

the operating conditions of long recycle delays and large air flow designed to minimize these effects.

The T_1 data have been analyzed as described under Materials and Methods section using two librational models about the $C_\alpha-C_\alpha$ axis. The relationship between amplitude, local correlation times, and T_1 relaxation time is illustrated in Figure 3 using the sweep model. For this figure the constants for the correlation functions, eqs 2 and 3, were calculated using the mean position of the N−H vectors seen in even numbered backbone sites (Ketchem et al., 1993), and the T_1 eq 6 was evaluated for a 4.7 T field strength. The surface described by contours in this figure represents the solution set for these equations. The minimum in this surface corresponds to a correlation time of 8 ns. The total librational amplitudes are known to be less than or equal to 20° from the observed chemical shifts, dipolar and quadrupolar interactions in aligned samples (Nicholson et al., 1991), and powder pattern averaging of the chemical shift tensors (Lazo et al., 1993, 1995). Therefore it can be concluded from this qualitative observation of efficient relaxation that there exists a correlation time for these local motions that is between 0.1 and 100 ns. The figure also demonstrates a high sensitivity to the amplitude and frequency variables near the observed T_1 time of approximately 3 s.

Shown in Figure 4 are specific contours of such a plot as that presented in Figure 3 for two different field strengths again using the sweep model. These have been generated using the 95% confidence error range as given in Figure 2. Data from 9.4 T experiments are presented as boxes, and the corresponding data at 4.7 T are presented as filled circles. The minima for these two curves are displaced significantly along the frequency axis as a result of the field strength difference. For all of these sites the solution sets for each field strength diverge on one side or the other of this minimum. Despite this, there is a substantial solution range for many of the sites that satisfies the data from both field strengths.

The analysis of the overlapped regions is presented in Figure 5. The filled circles represent the closest fit of the data as a function of motional amplitude. The circles basically follow the "dot in the box" solutions from Figure 4; however, they only describe the closest fit for each increment of the molecular amplitude and not solutions within experimental error. Also as a function of motional amplitude a sum of differences is calculated ($|T_{1obs}(4.7T) - T_{1calc}| + |T_{1obs}(9.4T) - T_{1calc}|$) and shown in the figure as a dashed line. This comparison of experimental and calculated T_1 values shows a distinct minimum for each residue that represents a best fit rms amplitude. When compared with the circles, a best fit local correlation time can be achieved. A third calculation is presented in this figure, a sum of the 60% confidence limits for the measured T_1 values, represented as a thin horizontal line. The overlap of the fringes of two distributions outside the 60% confidence limits represents less than a 5% probability, hence the use of 60% confidence limits. Therefore, the horizontal line represents the 95% confidence limit for the overlap of two distributions. The closest fit values that occur in the amplitude region where the sum of differences is less than the error limit represent the error range for the amplitude of these local motions. For most sites a narrow amplitude region occurs where the sum of differences is approximately an order of magnitude better than elsewhere. Gly_2 and Val_8 show broad minima in the sum of differences curve because there is considerable overlap in the curves (Figure 4) for these sites.

Figure 6 shows the Gly_2 and Leu_{12} amplitude versus correlation time curves for the wobble model to demonstrate the similarity of these results with the sweep model. The overlap of the curves for these two models is virtually identical. The frequency minima are the same, since the minima are dictated by the transition frequencies. However, the amplitude scale is different since the sweep model uses a Gaussian distribution while the wobble model uses a constant distribution in a square well potential. The best fit amplitudes are seen to be different for these two models by the curves for the sum of differences.

DISCUSSION

The efficient relaxation rates observed in the gramicidin backbone suggests the presence of nanosecond motions. The quantitative analysis of these rates as a function of residue number is shown in Figure 7. The best fits (minima of the sum of differences curve) for the librational frequencies of the various backbone sites using the sweep model are all within a factor of 5. The error range for the frequencies (i.e., the solution set below the error limit line) virtually overlaps for all residues studied. The frequency range from the wobble analysis for each residue virtually (within a factor of 2) overlaps with the error range of the sweep model for the same sites. There is excellent agreement between these models. Some site to site variation in amplitude or frequency was anticipated because of the variation in T_1 relaxation times shown in Figure 2. To be within a factor of 2 or 5 represents a very high degree of uniformity for the frequency of these nanosecond librational motions along the channel axis.

The sweep model yields essentially invariant rms amplitudes (approximately 6°) along the length of the channel (Figure 7). This uniformity may reflect the regularity in the channel structure which has recently been shown in the structure determination (Ketchem et al., 1993). In lipid bilayers the structure has been shown to be significantly more uniform than in SDS micelles (Arseniev et al., 1986; Lomize et al., 1992). The rms amplitude for the sweep model represents about 60% of the population distribution. For

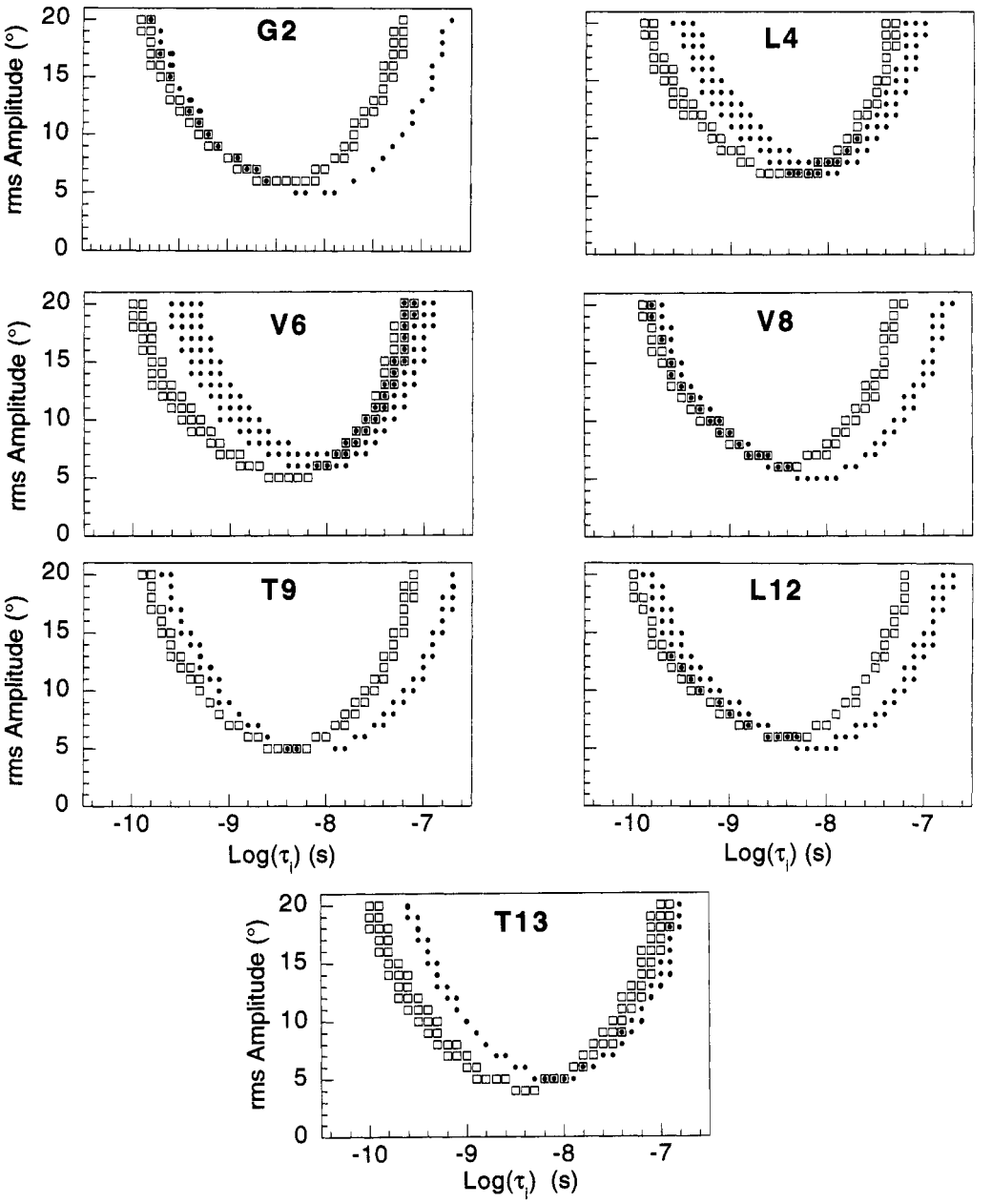

FIGURE 4: Local motional amplitude and frequency solution set for each residue using the sweep model at two different field strengths: 4.7 T (●), 9.4 T (□). The T_1 data are displayed with 95% confidence limits. The intersection of the two solution sets represents the amplitude and frequency parameters consistent with the entire solution set.

comparison, the square-well potential of the Gly_2 and Leu_{12} sites indicates a 9° semiangle amplitude for 100% of the population. Sixty percent of this population would be represented by a semiangle of 5.4° —virtually consistent with the Gaussian distribution of the sweep model. Therefore, the two motional models compared in this study yield very similar results. While additional models might be considered, they need to conform to the powder pattern results. Consequently, the motional models are significantly constrained, and within these constraints the analysis through the two models presented suggests that the conclusions with regard to frequency and amplitude are model independent. The spin−lattice relaxation rates for several backbone amide sites in oriented samples of the gramicidin channel at two different field strengths are consistent with motions of significant amplitude with characteristic times on the nanosecond time scale.

A number of studies have examined local motions in peptides using NMR. Correlation times for localized motions have been reported on time scales from picoseconds to nanoseconds. Correlation times for peptide backbone fluctuations on the nanosecond time scale have been reported by Cross and Opella (1982) in the fd bacteriophage coat protein. Using a restricted internal diffusion model and assuming a millisecond global correlation time for the interpretation of ^{13}C and ^{15}N T_1 and NOE measurements, local correlation times near 1 ns and motional amplitudes of 5° for a conical semiangle were determined. Sarkar et al. (1985) have also reported backbone motions on the nanosecond time scale in collagen. Here the motion was assumed to be an azimuthal rotational diffusion about the triple helical axis, but the authors did not speculate on the size of the molecular unit undergoing motion. More recently, Cole and Torchia (1991) have obtained field dependent T_1

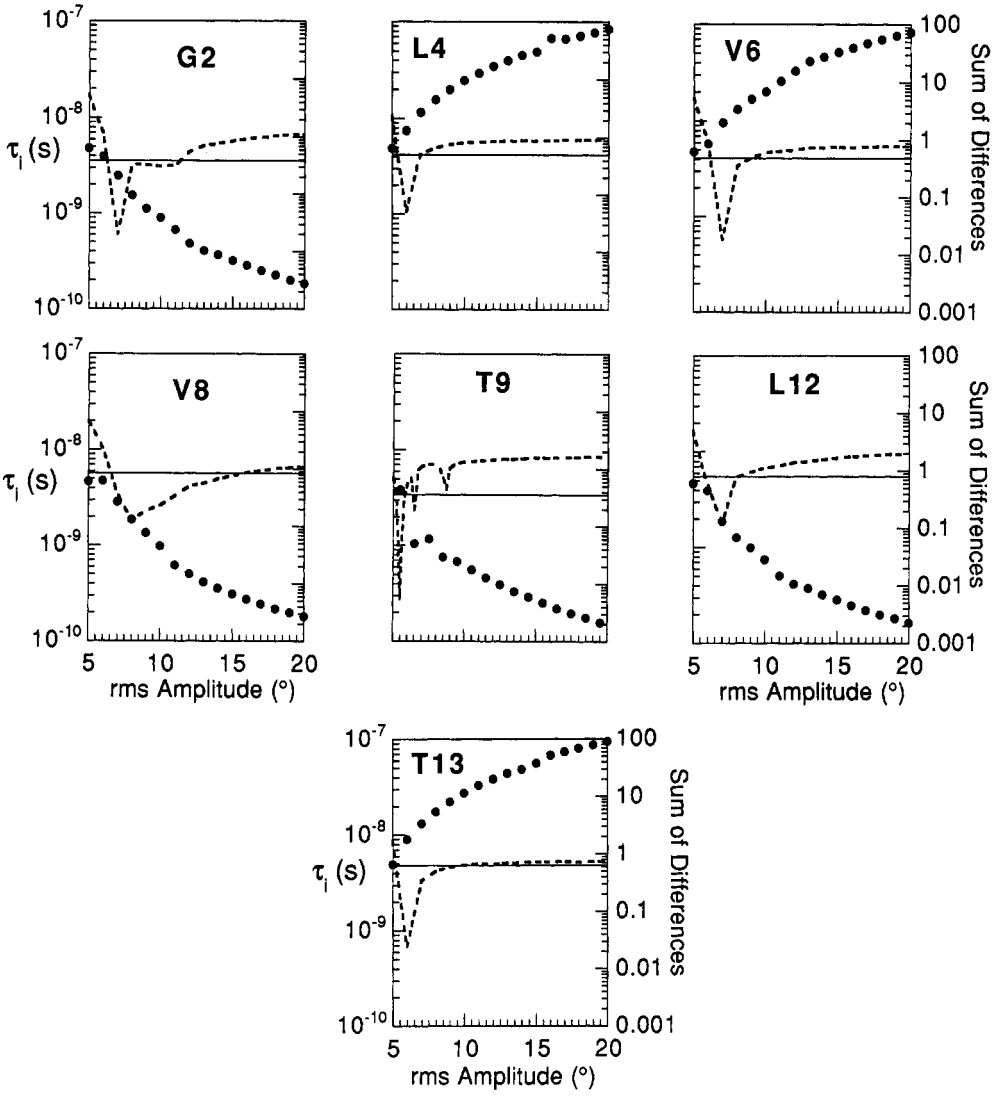

FIGURE 5: Best fit and error analysis for the T_1 results of the amide ^{15}N relaxation times presented in Figure 4. (●) Best-fit frequency for each rms amplitude. (- - -) Sum of differences between observed and calculated T_1 values. (—) is the 95% confidence limit for the overlap solution set.

data for the polypeptide backbone of staphylococcal nuclease in the crystalline state. Once again, the possibility of correlation times in the nanosecond or near-nanosecond time frame for local motion has been described.

Usha et al. (1991) have observed motions of peptide linkage planes in solid poly(benzyl glutamate) (PBG) using NMR to study deuterated amide nitrogen sites. By analyzing ^2H line shapes, they determined that the peptide planes librated about an axis parallel to the $C_\alpha-C_\alpha$ axis. They also showed that the root mean square libration was proportional to temperature, suggesting a harmonic potential, and at 300 K this amplitude was shown to be approximately 10°. An upper limit for the torsional frequency of a harmonic rotational oscillator with the moment of inertia of a single peptide plane rotating about the $C_\alpha-C_\alpha$ axis corresponds to a period of approximately 0.5 ps. Two models, restricted internal diffusion about an axis, and a damped harmonic oscillator were applied for the analysis of their T_1 data. The correlation time derived from this study for peptide plane librations is between 2.3 and 20 ps. The measured correlation times were compared with the upper limit torsional frequency to show that the peptide plane motion is highly overdamped in the α-helical PBG crystal.

Molecular dynamics simulations and a normal mode calculation of the gramicidin backbone dynamics have described librational motions on time scales three orders of magnitude shorter than the time frame observed here. This has generated an apparent discrepancy between the computational and experimental results. However, due to computational limitations, molecular dynamics trajectories have not sampled the nanosecond time scale nor have they reproduced a spontaneous ion translocation through the channel. Furthermore, in the presence of nanosecond molecular motions, the relaxation techniques of this study would be insensitive to motions on the picosecond range. Since spin—lattice relaxation is most sensitive to molecular motions occurring on a time scale near the Larmor frequencies of the coupled nuclei, the presence of motional rates in this regime will obscure the effects of much faster motions. Therefore, the observation of nanosecond motions does not rule out the presence of picosecond motions. Moreover, the frequency independent (actually frequencies greater than 100 kHz) librational amplitudes obtained from powder pattern averaging are considerably larger (±20°) than the amplitudes fit by the relaxation properties described here (±6°). Powder pattern analysis of librational frequencies is therefore a linear

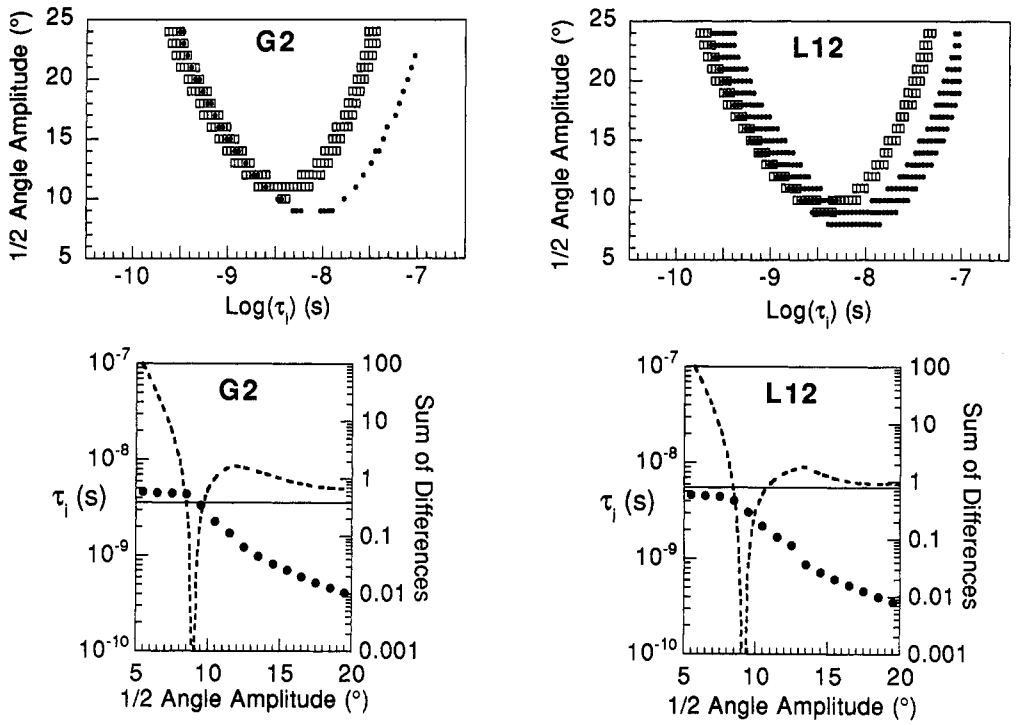

FIGURE 6: Local motional amplitude and frequency solution as in Figure 4 except that the wobble model is used and only Gly_2 and Leu_{12} are shown as examples. Below is shown the best fit and error analysis for these solutions. The analysis is presented in Figure 5.

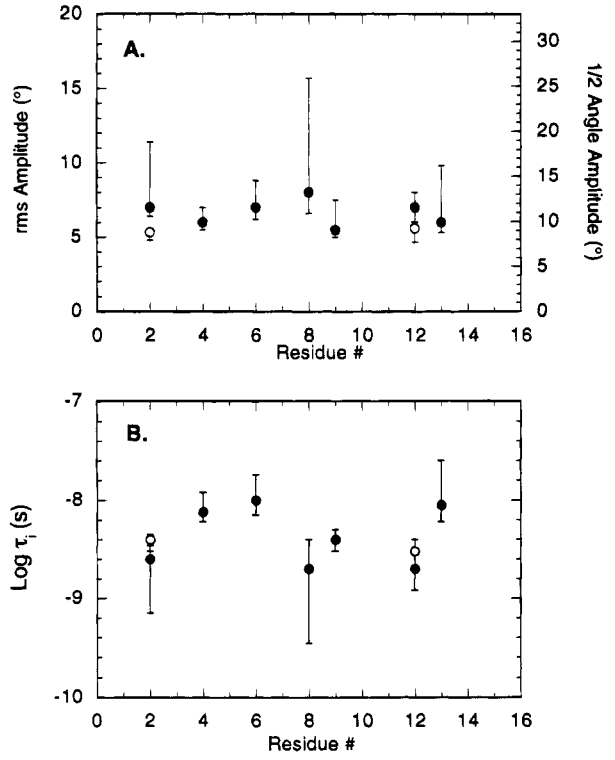

FIGURE 7: Plot of the amplitude and frequency range between error bars for each residue using the sweep model (●) and for Gly_2 and Leu_{12} using both the sweep (●) and wobble (○) models. The overall best fit is also shown with the filled and open circles.

detector for all frequencies greater than 10^5 Hz, whereas the relaxation analysis is very much a nonlinear detection devise for librational frequencies. The powder pattern analysis is seeing a combination of the relaxation sensitive motions and librational motions on the other time scales, presumably the picosecond time scale. The presence of significant librational amplitudes in the picosecond time frame would reduce the apparent conflict between the relaxation results and the molecular dynamics calculations.

The molecular dynamics simulations suggest that the backbone is sufficiently dynamic to support librational amplitudes that are consistent with the results of this research. Of particular interest are the implications of the molecular dynamics/free energy profile study by Roux and Karplus (1991a,b) on an infinite periodic poly(L,D-alanine) model of the gramicidin channel interior. The surrounding structure was considerably perturbed by the presence of an ion, and this suggested the presence of correlated librations among the peptide planes in the ion solvation environment. They suggest that an ion should not be thought of as hopping between separate energy minima, rather that the local energy minima flows with the ion. Roux and Karplus (1991b) have stated that more extensive correlations in gramicidin would not be favored because of the high degree of flexibility in the backbone. However, the backbone is much less flexible than these authors predicted. Although the tensor averaging of Lazo et al. (1993) has shown librational amplitudes up to ±20°, the effect of cations on the structure and dynamics is very small (Separovic et al., 1994; Ketchem et al., 1994), on the order of a few degrees instead of 20° or more as suggested by Roux and Karplus (1991b). In other words, the cations do not induce large deformations in the backbone conformation or large changes in dynamic amplitudes; consequently, the backbone lacks the flexibility suggested by the computational study and, therefore, more extensive motional correlations can be anticipated.

For local motions to be overdamped into the nanosecond time scale, the extent of the oscillating unit and the involved moment needs to be much greater than that of a single peptide plane. Local viscosity damps high frequency librations of an oscillating unit, but it is unlikely that local viscosity or "solvent" effects alone would overdamp the local motions by several orders of magnitude. If the local motions

are correlated, the rotational moment of the oscillating unit would be increased resulting in substantial slowing of the librational frequency. Not only have molecular dynamics calculations suggested limited correlated motions, but in a molecular mechanics study Venkatachalam and Urry (1984) suggested that the entire gramicidin A helix might librate in unison, a dynamic process they called "helical librations".

Actually, correlated motions are known to exist in the channel, in that all molecules and ions in the channel must move in unison in order to migrate through the channel, because the molecules and ions are restricted to a single file column. Consequently, the question is not whether or not correlated motions exist in the gramicidin channel, but only whether they extend to the polypeptide itself and, if so, how extensive are the correlations.

Andersen (1983) reported a voltage independent single channel current for gramicidin A of 2.7 pA at voltages up to 500 mV. This corresponds to approximately 60 ns for an ion to pass through the channel. It has been estimated on the basis of energetics (Roux & Karplus, 1991a) that the average time spent in each potential well separated by a dipeptide unit is 10 ns. And Becker et al. (1992) have reported that by fitting the large amount of kinetic data available to a detailed four-state model that the rate constant for Na^+ ions jumping between the two binding sites at either end of the channel is $7 \times 10^6\ s^{-1}$. This is equivalent to one translocation per 142 ns or 12 ns per pair of residues between the binding sites near the Trp_{11} carbonyl. The observation of local motions on the nanosecond time scale raises the very exciting possibility that a direct correlation exists between the molecular dynamics of the backbone and the functional process of a cation translating through the channel.

A variety of models for correlated motions can be envisioned that would overdamp the librational frequencies. The gramicidin structure is both dynamic and stiff; in other words, it is hard to deform. Therefore, once a deformation is induced in the structure, it could be expected to propagate throughout the molecule. There are three types of collective modes that could lead to substantially increased moments for the motions of the polypeptide backbone. First, correlation among the peptide planes as previously suggested by the computational studies. Second, correlations from the backbone to the relatively high viscosity lipid environment through the amino acid side chain. Third, a global deformation of the helical structure induced by interactions between the lipid molecules and the indole sidechains.

Correlated motions among the peptide planes could be mediated by one or a combination of several mechanisms. The covalent bonds to the C_α carbon that joins adjacent peptide planes could provide a mechanism. Correlation of near neighbors and the fact that in a β-sheet type of structure the repeat unit is a dipeptide suggests sequential correlations along the length of the polypeptide chain (Figure 8A). Furthermore, to maintain the helical parameters while having substantial local motions, extensive correlations among the neighboring peptide planes must occur. Correlations in the backbone could, therefore, be mediated by the interaction energy associated with the covalent linking of the peptide planes (i.e., the bonds to the C_α carbons).

Alternatively, the interaction energy associated with the hydrogen bonds between peptide planes could mediate the correlated motions in the backbone. The residues of the gramicidin channel helix are each hydrogen bonded to their

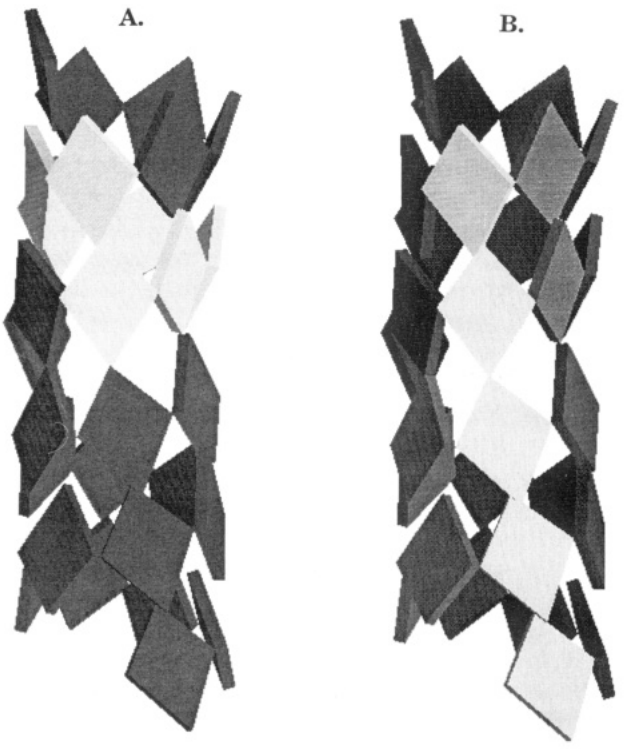

FIGURE 8: Representation of the gramicidin channel backbone structure (Ketchem et al., 1993) using the GRASP program developed by Anthony Nichols (Columbia University). Each peptide linkage is represented by a plane suggesting only limited flexibility about the $C_\alpha - C_\alpha$ axis. (A) A single turn of the helix is highlighted representing a model for correlated motions mediated by the covalent connections between peptide planes. (B) A stripe of peptide planes connected by hydrogen bonds representing another mechanism for correlated between peptide planes.

sixth neighbor. Thus individual residues are well connected to distant neighbors along the channel. In this manner, columns of peptide planes that are approximately parallel to the channel axis may be correlated (Figure 8B). Each column possesses a relatively uniform collection of peptide plane orientations.

Thirdly, it is possible that the correlated motions could be mediated by electrostatic interactions, such as dipole–dipole or monopole–dipole interactions. Molecular dynamics calculations have predicted the formation of bifurcated hydrogen bonds between the carbonyl oxygens and the water molecules (Chiu et al., 1989). Similarly, the solvation of the cations in the channel have been modeled with the simultaneous perturbation of four carbonyl groups by the ions (Roux & Karplus, 1991b). The motion of either cation or water molecules in the channel could promote collective motions in the backbone.

The motions of the peptide linkages could be correlated with motions of the side chains in the relatively high viscosity lipid environment. Correlations that are constrained to be within individual residues are quite unlikely. The observed dynamics in the backbone are very uniform, a result that might not be anticipated from individual correlated domains. Lee et al. (1995) described an apparent dynamic phase boundary between the lipid and the peptide, and, consequently, the effects of the lipid environment in this regard are not anticipated to be very substantial although it is known that a change in the lipid phase dramatically changes the conductance of the channel (Krasne et al., 1971). In addition, the side chains show very limited dynamics; the only residues

having large amplitude dynamics other than methyl jumps are the χ_1 motions of the Val_1 and Val_7 residues (Lee & Cross, 1994; Lee et al., 1995). If the individual correlated domains were not isolated but in some way coupled, then side chain correlations would become a more likely mechanism. In fact, the coupling of the χ_1 dynamics of Val_1 and Val_7 has been suggested since these two residues pack closely together on the surface of the channel. However, such opportunities for forming sidechain correlation domains appear to be rare at the gramicidin/lipid interface.

There is another intriguing possibility. Side chains could act as lever arms transmitting torque from the solvent to the peptide backbone. Local changes in the helical parameters could be induced by collisions between diffusing lipid molecules and the relatively rigid indole rings of the carboxy terminus. The effect of this torque can be visualized by stretching out three turns of a "Slinky" and twisting the top and/or bottom turn. The plane of the spring helix can be seen to librate in response to the torque. By implicating the whole molecular system in the local motions, two conditions which provide for the slowing of a rotational harmonic oscillator are met: the size of the oscillating unit and the involved mass are increased. However, the uniformity of these nanosecond motions along the length of the channel are not easily accounted for by such a model.

Possibilities for correlations in the dynamics of the peptide planes are considerable and generate major challenges for both experimentalists and computationalists. The prospect of a direct correlation between kinetics and dynamics counters the long-standing hypothesis that a bound cation is only able to experience time-averaged structures and, therefore, time-averaged potentials. The presence of motions on the nanosecond time scale indicates that a bound cation experiences a fluctuating structure and a local potential which fluctuates on the time scale of cation translocation, hence the intriguing possibility of a correlation between local dynamics and channel conductance. Such correlations could help to explain the remarkable efficiency with which the gramicidin channel functions. Similar dynamics/function correlations may be important in many membrane proteins.

ACKNOWLEDGMENT

We are indebted to the staff of the FSU NMR facility: J. Vaughn, R. Rosanske, and T. Gedris for their skillful maintenance, modification, and service of the NMR spectrometers and Hank Henricks and Umesh Goli in the Bioanalytical Synthesis and Services Facility for their expertise and maintenance of the ABI 430A peptide synthesizer and HPLC equipment.

REFERENCES

Abragam, A. (1961) in *Principles of Nuclear Magnetism*, Clarendon, Oxford.
Andersen, O. S. (1983) *Biophys. J. 41*, 119−133.
Arseniev, A. S., Barsukov, I. L., Bystrov, V. F. (1986) in *Chemistry of Peptides and Proteins* (Voelter, W., Bayer, E., Ovchinnikov, Y. A., & Ivanov, V. T., Eds.) Vol. 3, pp 127−158, Walter de Gryter and Co., Berlin.
Becker, M. D., Koeppe, R. E., II, & Andersen, O. S. (1992) *Biophys. J. 62*, 25−27.
Brooks, B., & Karplus, M. (1983) *Proc. Natl. Acad. Sci. U.S.A. 80*, 6571−6575.
Bull, T. E. (1978) *J. Magn. Reson. 31*, 453−458.
Busath, D. (1993) *Annu. Rev. Physiol. 55*, 473−501.
Busath, D., & Szabo, G. (1981) *Nature 294*, 371−373.
Chandrasekhar, S. (1943) *Rev. Mod. Phys. 15*, 1−87.
Chiu, S.-W., & Jakobson, E. (1993) *Biophys. J. 64*, A301.
Chiu, S.-W., Subramaniam, S., Jakobsson, E., & McCammon, J. A. (1989) *Biophys. J. 56*, 253−261.
Chiu, S.-W., Jakobsson, E., Subramaniam, S., & Mccammon, J. A. (1991) *Biophys. J. 60*, 273−285.
Chiu, S.-W., Novotny, J. A., & Jakobsson, E. (1993) *Biophys. J. 64*, 98−108.
Cole, H. B. R., & Torchia, D. A. (1991) *Chem. Phys. 158*, 271.
Cross, T. A. (1994) *Annu. Rev. NMR Spectrosc. 29*, 123−167.
Cross, T. A., & Opella, S. J. (1982) *J. Mol. Biol. 159*, 543−549.
Cross, T. A., Ketchem, R. R., Hu, W., Lee, K.-C., Lazo, N. D., & North, C. L. (1992) *Bull. Magn. Reson. 14*, 96−101.
Evans, J. N. S., Appelyard, R. J., & Shuttleworth, R. J. (1993) *J. Am. Chem. Soc. 115*, 1588−1590.
Fields, C. G., Fields, G. B., Noble, R. L., & Cross, T. A. (1989) *Int. J. Pept. Protein Res. 33*, 298−303.
Fields, G. B., Fields, C. G., Petefish, J., Wart, H. E. V., & Cross, T. A. (1988) *Proc. Natl. Acad. Sci. U.S.A. 85*, 1384−1388.
Fonseca, V., Daumas, P., Ranjalahy-Rasoloarijao, L., Heitz, F., Lazaro, R., Trudelle, Y., & Andersen, O. S. (1992) *Biochemistry 31*, 5340−5350.
Harold, F. M., & Baarada, J. R. (1967) *J. Bacteriol. 94*, 53−60.
Hu, W. (1994) Doctoral Dissertation, Florida State University, Tallahassee, FL.
Hu, W., Lee, K.-C., & Cross, T. A. (1993) *Biochemistry 32*, 7035−7047.
Jordan, P. C. (1987) *J. Phys. Chem. 91*, 6582−6591.
Ketchem, R. R., Hu, W., & Cross, T. A. (1993) *Science 261*, 1457−1460.
Ketchem, R. R., Hu, W., Tian, F., & Cross, T. A. (1994) *Structure 2*, 699−701.
Killian, J. A. (1992) *Biochim. Biophys. Acta 1113*, 391−425.
Koeppe, R. E., II, Mazet, J.-L., & Andersen, O. S. (1990) *Biochemistry 29*, 512−520.
Koeppe, R. E., II, Killian, J. A., & Greathouse, D. V. (1994) *Biophys. J. 66*, 14−24.
Krasne, S., Eisenman, G., & Szabo, G. (1971) *Science 174*, 412−415.
Lazo, N., Hu, W., Lee, K.-C., & Cross, T. A. (1993) *Biochem. Biophys. Res. Commun. 197*, 904−909.
Lazo, N. D., Hu, W., & Cross, T. A. (1995) *J. Magn. Reson. 106B* (in press).
Lee, K.-C. (1994) Doctoral Dissertation, Florida State University, Tallahassee, FL.
Lee, K.-C., & Cross, T. A. (1994) *Biophys. J. 66*, 1380−1387.
Lee, K.-C., Hu, W., & Cross, T. A. (1993) *Biophys. J. 65*, 1162−1167.
Lee, K.-C., Huo, S., & Cross, T. A. (1995) *Biochemistry 34*, 857−867.
Lee, W. K., & Jordan, P. C. (1984) *Biophys. J. 46*, 805−819.
Lipari, G., & Szabo, A. (1981) *J. Chem. Phys. 75*, 2971−2976.
Lipari, G., & Szabo, A. (1982a) *J. Am. Chem. Soc. 104*, 4546−4559.
Lipari, G., & Szabo, A. (1982b) *J. Am. Chem. Soc. 104*, 4559−4570.
Lomize, A. L., Orechov, V. Yu., & Arseniev, A. S. (1992) *Bioorg. Khim. 18*, 182.
London, R. E. (1980) in *Magnetic Resonance in Biology* (Cohen, J. S., Ed.) Wiley, New York.
Macdonald, P. M., & Seelig, J. (1988) *Biochemistry 27*, 2357−2364.
Mackay, D. H. J., Berens, P. H., Wilson, K. R., & Hagler, A. T. (1984) *Biophys. J. 46*, 229−48.
McCammon, J. A., & Harvey, S. C. (1987) in *Dynamics of Protein and Nucleic Acids*, Cambridge University Press, New York.
Moll, F., III and Cross, T. A. (1990) *Biophys. J. 57*, 351−362.
Nicholson, L. K., & Cross, T. A. (1989) *Biochemistry 28*, 9379−9385.
Nicholson, L. K., Moll, F., Mixon, T. E., Lograsso, P. V., Lay, J. C., & Cross, T. A. (1987) *Biochemistry 26*, 6621−6626.
Nicholson, L. K., Teng, Q., & Cross, T. A. (1991) *J. Mol. Biol. 218*, 621−637.
North, C. L., & Cross, T. A. (1993) *J. Magn. Reson. 101B*, 35−43.

Roux, B., & Karplus, M. (1988) *Biophys. J. 53*, 297−309.
Roux, B., & Karplus, M. (1991a) *J. Phys. Chem. 95*, 4856−4868.
Roux, B., & Karplus, M. (1991b) *Biophys. J. 59*, 961−981.
Sarges, R., & Witkop, B. (1965) *J. Am. Chem. Soc. 87*, 2011−2020.
Sarkar, S. K., Sullivan, C. E., & Torchia, D. A. (1985) *Biochemistry 24*, 2348.
Separovic, F., Gehrmann, J., Milne, T., Cornell, B. A., Lin, S. Y., & Smith, R. (1994) *Biophys. J. 67*, 1495−1500.
Smith, R., & Cornell, B. A. (1986) *Biophys. J. 49*, 117−118.
Smith, R., Thomas, D. E., Separovic, F., Atkins, A. R., & Cornell, B. A. (1989) *Biophys. J. 56*, 307−314.
Sung, S. S., & Jordan, P. C. (1987a) *Biophys. Chem. 27*, 1−6.
Sung, S. S., & Jordan, P. C. (1987b) *Biophys. J. 51*, 661−672.
Teng, Q., & Cross, T. A. (1989) *J. Magn. Reson. 85* 439−447.
Torchia, D. A. (1978) *J. Magn. Reson. 30*, 613−616.
Torchia, D. A., & Szabo, A. (1982) *J. Magn. Reson. 49*, 107−121.
Urry, D. W. (1971) *Proc. Natl. Acad. Sci. U.S.A. 68*, 672−676.
Urry, D. W., Venkatachalam, C. M., Prasad, K. U., Bradley, R. J., Parenti-Castelli, G., & Lenaz, G. (1981) *Int. J. Quantum Chem., Quantum Biol. Symp. 8*, 385−399.
Urry, D. W., Venkatachalam, C. M., Wood, S. A., & Prasad, K. U. (1985) *Struct. Motion: Membr. Nucleic Acids Proteins, Proc. Int. Symp. Struct. Dyn. Membr. Nucleic Acids Proteins*, 185−203.
Usha, M. G., Peticolas, W. L., & Wittebort, R. J. (1991) *Biochemistry 30*, 3955−3962.
Venkatachalam, C. M., & Urry, D. W. (1984) *J. Comput. Chem. 5*, 64−71.
Woolf, T. B., & Roux, B. (1994) *Proc. Natl. Acad. Sci. U.S.A. 91*, 11631−11635.
Woolf, T. B., Desharnais, J., & Roux, B. (1994) *NATO Advanced Workshop on Supramolecular Chemistry* (Wippf, G., Ed) pp 519−531, Kluwer Academic Publishers, Dordrecht, The Netherlands.

BI942618P